



Geological and Geotechnical Characteristics of London Clay from the Isle of Sheppey

Meghdad Bagheri · Mohammad Rezania

Received: 13 January 2020 / Accepted: 16 September 2020
© The Author(s) 2020

Abstract The paper describes a series of experimental testing on natural stiff London clay samples retrieved from the New Hook Farm in the Isle of Sheppey, UK. The experimental program includes determination of macroscopic and microscopic properties, chemical compositions, Atterberg limits, permeability, and compressibility parameters in both intact and reconstituted states. The paper integrates the earlier studies, the new findings, and the commercial investigation results with the aim to extend the current knowledge of the geological and geotechnical characteristics of this stiff clay from the east of the London basin. Some comparisons are also made with shallow depth London clay from Heathrow Terminal 5 site.

Keywords Clays · Compressibility · Grain size analysis · Microstructure

List of Symbols

A Specimen cross section area
 C_c Compression index

C_s Swelling index
 C_α Creep index
 D Particle diameter
 D_{10} The intercept for 10% cumulative mass on PSD curve
 D_{25} The intercept for 25% cumulative mass on PSD curve
 D_{50} The intercept for 50% cumulative mass on PSD curve
 D_{75} The intercept for 75% cumulative mass on PSD curve
 D_{90} The intercept for 90% cumulative mass on PSD curve
 e Void ratio
 e_0 Initial void ratio
 G_s Specific gravity
 i Hydraulic conductivity
 I_p Plasticity index
 k_v COEFFICIENT of vertical permeability
 p' Mean effective stress
 p_c Pressure loss in the specimen
 Q Mean rate of flow of water through the soil specimen
 q/p' Stress ratio
 q Deviatoric stress
 R_t Temperature correction factor for the viscosity of water
 S_0 Initial suction
 w_0 Initial gravimetric water content
 w_L Liquid limit

M. Bagheri
School of Energy, Construction and Environment,
Coventry University, Coventry, UK
e-mail: meghdad.bagheri@coventry.ac.uk

M. Rezania (✉)
School of Engineering, University of Warwick, Coventry,
UK
e-mail: m.rezania@warwick.ac.uk

w_p	Plastic limit
α	Represents the ratio C_{α}/C_c
ρ_b	Initial bulk density
σ_p	Yield vertical net stress
σ'_v	Vertical effective stress
σ_{vnet}	Vertical net stress
ε_a	Axial strain
ESEM	Environmental Scanning Electron Microscope
EDX	Energy dispersive X-ray
LC	London clay
MCV	Moisture condition value
PSD	Particle size distribution
QD	Queensborough clay
SWRC	Soil water retention curve
T5	Terminal 5 site
TDS	Total dissolved solids
WAC	Waste acceptance criteria

1 Introduction

Since 1960s, the Isle of Sheppey along with the Isle of Grain, Cliffe, and Foulness Island have been labelled as potential sites for construction of a new airport as an alternative to the Heathrow airport to reduce the aircraft noise pollution in south east of England (Helsey and Codd 2014). The proposals of new airport in the Isle of Sheppey, the birthplace of British aviation, although rejected several times by the Department for Transport, implies the significance of this site which may in future be considered for wider infrastructure investments and developments. The ground profile of the Isle of Sheppey consists of deep London clay (LC) deposits. Very few works can be found in the literature on characterisation of the Sheppey LC (e.g. Burnett and Fookes 1974; Huggett 1994), despite the necessity for developing a clear understanding of the geological and hydro-mechanical properties of this soil. In one of the few studies on Sheppey soils, Jardine et al. (2003) reported characterisation of a soft peaty clay deposit found at the Queensborough bypass viaduct site on the north of the Isle of Sheppey. This temperate estuarine marsh clay is known as Queensborough clay (QC) and has been the subject of several studies (e.g. Smith 1992). The QC was reported to be mixed with material from

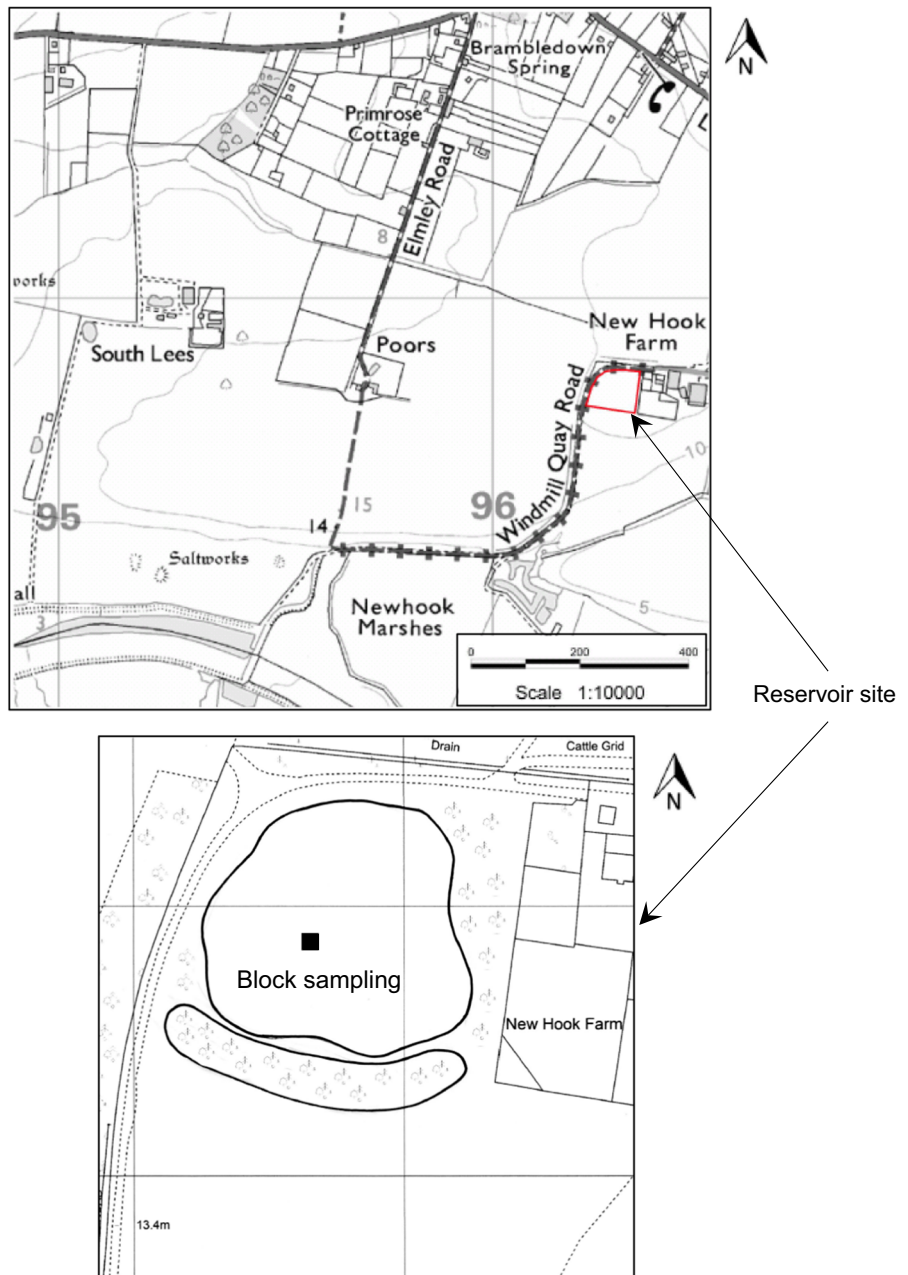
surrounding LC hills and cliffs as a result of mass movement and sea erosion (Jardine et al. 2003). The reconstituted QC was found to have identical Atterberg limits, grading curve, and intrinsic compression parameters to the reconstituted LC samples investigated and reported by Jardine (1985). Hence, still there appears to be a lack of technical knowledge on characteristics of the Sheppey LC. An experimental program was, therefore, devised to fill this gap and add valuable information to the existing database. Undisturbed block samples of 350 mm cube were taken at 4 m depth below non-quarried ground level at New Hook farm reservoir site located on the outskirts of Sheerness town on the Isle of Sheppey. This site is owned by SW Attwood & Partners Ltd. The principal operation of the site is a fishing pond and water reservoir and at the time of sampling, it was in its initial stages of excavation. Figure 1 presents the site map and location of block sampling.

Commercial laboratory testing was carried out by CET Structures Ltd and included contamination analysis, permeability and in-situ water content measurements. Preliminary laboratory testing for microstructural analysis and determination of the index properties, chemical composition, and one-dimensional compressibility were carried out at the University of Nottingham and The University of Warwick. The obtained results are compared with the corresponding characteristics of the shallow depth LC from Terminal 5 (T5) site at Heathrow airport, reported in the literature.

2 The Sheppey Member

King (1981) studied the biostratigraphy and lithological variations of LC formation and suggested a division of the formation into five principal units, named Divisions A to E. These divisions are subdivided into several members within the LC formation, named as; Walton, Claygate, Ockendon, Avey, Sheppey, and Bracknell Members. The LC formation in Sheppey cliffs, Isle of Sheppey, which exposes the upper part of the LC formation is named Sheppey Member and corresponds approximately to the upper part of Division C, Division D and most of Division E (King 1981). The thickness of the Sheppey Member is approximately 55 m and is classified as Thames Group. According to Aldiss (2014), the Sheppey

Fig. 1 Site map and sampling locations in New Hook farm



Member mainly comprises silty clay diffusely interbedded with sandy clayey silt and contains several layers of calcareous concretions.

Burnett and Fookes (1974) reported that the Sheppey LC comprises of 58% of particles $< 2 \mu\text{m}$ size and 42% particles $> 2 \mu\text{m}$ size. The particles $< 2 \mu\text{m}$ size were approximately 90% clay minerals which were found to comprise 57% montmorillonite (a

member of smectite group), 24% illite, 12% kaolinite, and 7% chlorite. The particles $> 2 \mu\text{m}$ size were mainly silt which was found to comprise 70% quartz carbonates, 15% pyrite, and 15% clay minerals. Similar compositions were reported by Gasparre (2005) for Unit C (7 m depth) T5 LC, which comprises 53% of particles $< 2 \mu\text{m}$ size formed mainly of 60%

illite–smectite, 22% illite, 15% kaolinite, and 4% chlorite.

3 Macro-Fabric and Microstructure

The macro-fabric of LC is characterised by the presence of discontinuities which play a significant role in its mechanical behaviour (Burland 1990; Hight and Jardine 1993; Hight et al. 2003). These discontinuities are in the form of fissures, joints (or backs), bedding surfaces (or laminations), tectonic shear surfaces, recently formed shear surfaces, and minor faults (Skempton et al. 1969; Hight et al. 2003). Figure 2 depicts the fissured and jointed pattern of the LC at shallow depth at New Hook farm and T5 sites. The occurrence of fissures was reported to be the dominant feature of the block samples retrieved from Unit C (7 m depth) at T5 site (Gasparre 2005).

The brown, brownish grey, or mottled brown and grey coloured LC, typically found in the top 5–10 m depths, has been recognised as weathered LC (colour changes from blue-grey to brown) and contains selenite crystals, a form of gypsum-hydrated calcium sulphate (Hight et al. 1993; Aldiss 2014). Figure 3 shows the presence of selenite crystals in retrieved samples from New Hook farm.

To identify the basic structural properties (soil fabric) and chemical composition of the retrieved samples, a microstructure and mineralogy analysis was carried out using a Philips XL30 FEG environmental scanning electron microscope (ESEM) equipped with an Energy Dispersive X-ray (EDX) analyser. For ESEM analysis, cubic subsamples of approximately 1 cm³ size were excavated from the central portions of the intact samples.

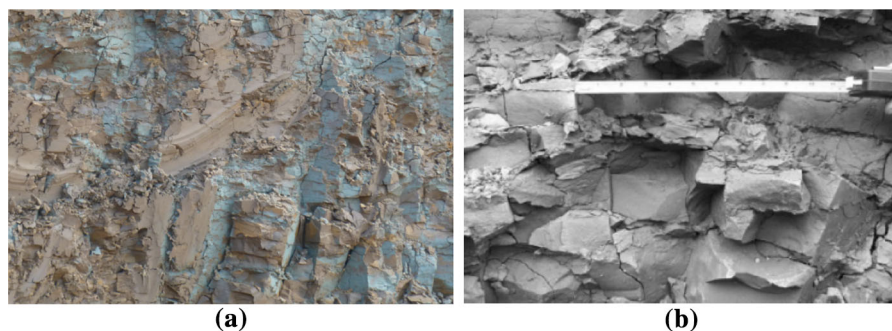


Fig. 2 Fissured pattern at: **a** shallow depth at New Hook farm reservoir site; **b** shallow depth at T5 site (Hight et al. 2007)

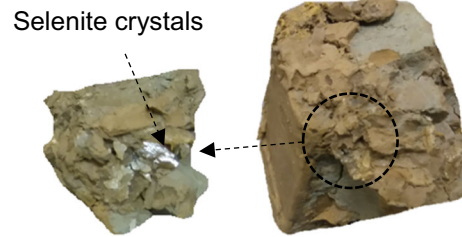


Fig. 3 Selenite crystals found in retrieved samples

The micrographs of Figs. 4 and 5 reveal the large proportions of randomly oriented silt with irregular angular fine sand-sized grains and calcite crystals imbedded in the clay matrix.

The clay structure appears to be flocculated and composed of proportionally equal large flocs and single plate-shaped particles with edge-to-edge, edge-to-face and face-to-face contacts (Fig. 6). As can be seen, the edge-to-edge contacts of the clay domains have resulted in development of large pores in the clay cluster. This soil fabric is comparable with flocculated cardhouse fabric reported by Gasparre (2005) for T5 LC at shallow depths. The micrograph of Fig. 7 depicts a pyrite particle surrounded by clay domains and single particles.

Figure 8 shows the steps of drying a flooded specimen in the ESEM. As can be seen, the drying process does not noticeably affect the macrostructure and arrangement of the clay flocs. Also shown in the figure, is the removal of the water menisci developed at inter-floc pores (throats) during sequential drying of the specimen.

4 Chemical Composition

The diagenesis analysis carried out by Huggett (1994) on LC samples recovered from Warden Point on the

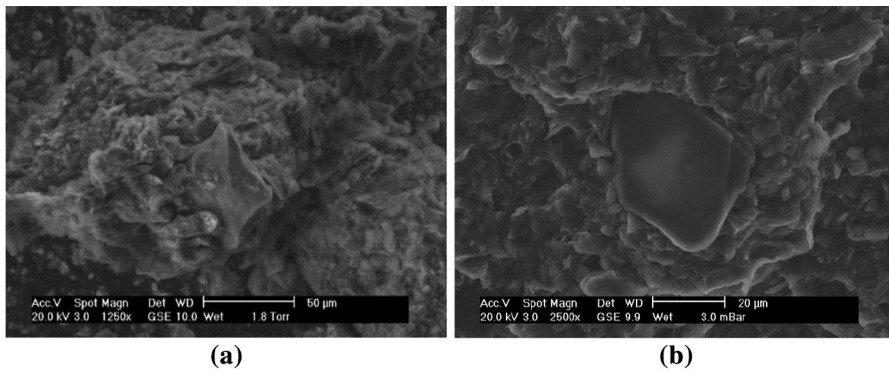


Fig. 4 ESEM micrographs showing the coarser-grained particles imbedded in the clay matrix at magnification of: **a** 1250x, **b** 2500x

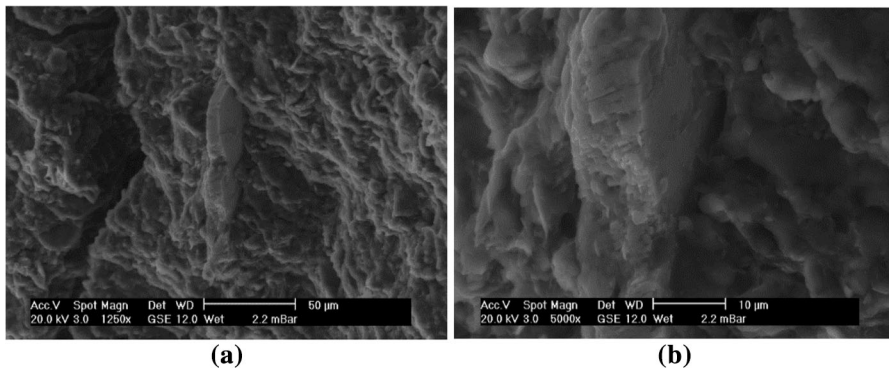


Fig. 5 ESEM micrographs showing the oriented fabric, fracture through the sample, and calcite crystal between clay grains and clay particles at magnification of: **a** 1250x; **b** 5000x



Fig. 6 ESEM micrograph: **a** soil fabric, **b** schematic diagram of particles and domains arrangements and presence of large pores in flocculated soil fabric

Isle of Sheppey, revealed the similarity in compositions of Sheppey LC with Ockenden LC, with differences being only in the relative proportions of some diagenetic minerals. The principal authigenic minerals in Sheppey LC are carbonates, apatite and pyrite. The fibrous calcite, present in Sheppey

concretions, comprises a maximum of 5% total Magnesium (Mg), Manganese (Mn), and Iron (Fe). About 50% of the concretions comprise predominantly detrital clay minerals of illite and smectite, with the presence of a slight amount of coarsely crystalline authigenic kaolinite. Silt grains are predominantly

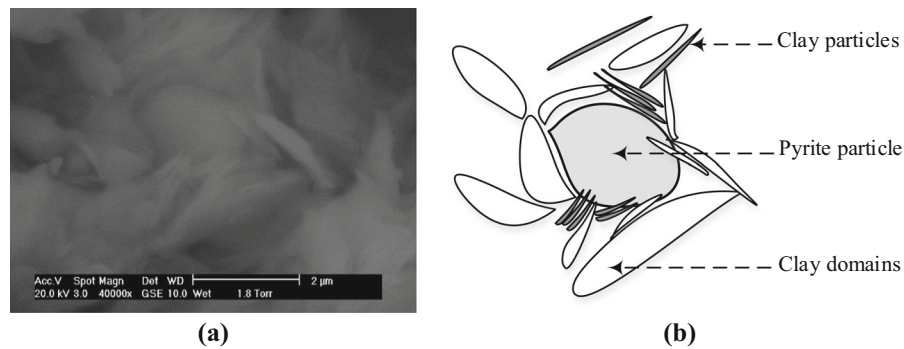
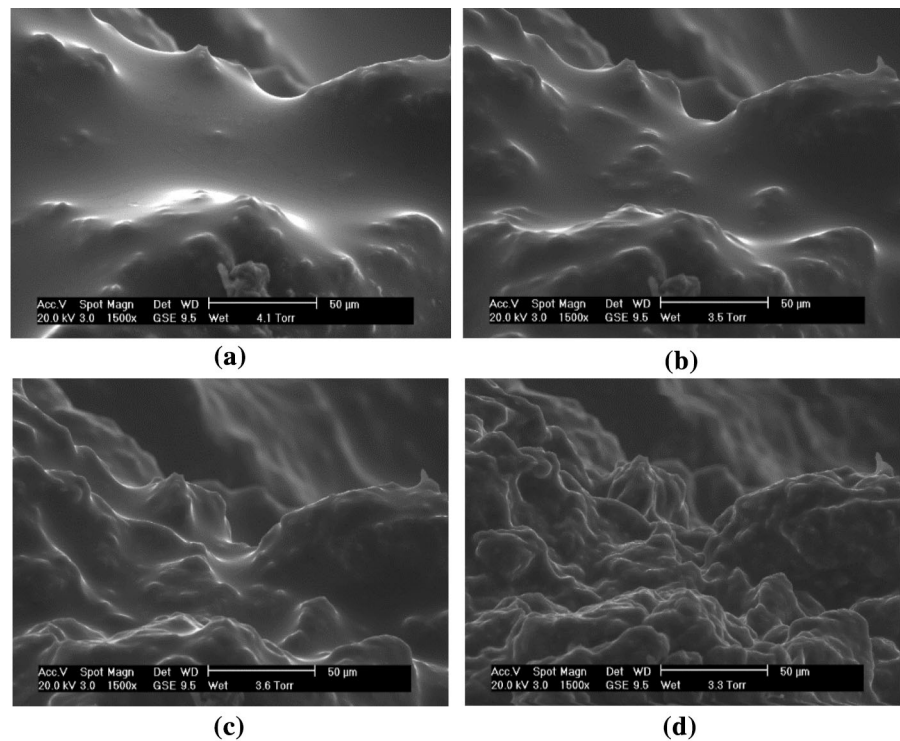


Fig. 7 Clay particles and domains around a pyrite particle: **a** ESEM micrograph, **b** schematic diagram

Fig. 8 ESEM micrographs showing the progressive drying of the clay sample



quartz and K-feldspar. A clay/quartz ratio of 3.2:1 was also reported. Similar results were obtained from the EDX analysis carried out in this research, as shown in Fig. 9. The key petrographical characteristics of the sample are summarised in Table 1. It is observed that Silicon dioxide (SiO_2), Aluminium oxide (Al_2O_3), Calcium carbonate (CaCO_3), and Iron disulphide (FeS_2) are predominant constituents of the samples. Calcium (Ca) and Iron are the products of weathering of silicate minerals. Calcium carbonate precipitates are formed from the chemical interaction of Calcium and Carbon Dioxide (CO_2) molecules dissolved in sea

water. Similarly, Iron reacts with Sulphur (S), resulting from rotting organic matter, and forms pyrite (FeS_2) (Gasparre 2005).

The waste acceptance criteria (WAC) testing was carried out by CET Structures Ltd on representative samples taken from the reservoir site to determine if the soil (waste) has any hazardous properties as per the Environment Agency's Hazardous Waste Technical Guidance WM2. The likely behaviour of waste in a landfill is assessed against WAC limits for granular waste acceptance at inert waste landfills, stable non-reactive hazardous landfills, and hazardous waste

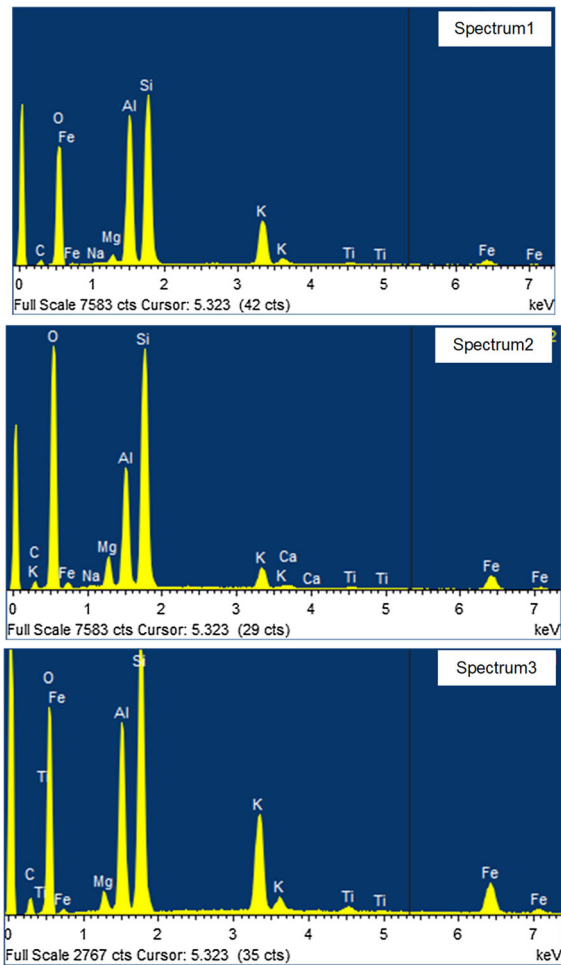


Fig. 9 The X-Ray spectra acquired from different points on the same sample

Table 1 Average chemical composition (% by weight) of Sheppey LC

Spectrum	C (CaCO ₃)	O (SiO ₂)	Na (Albite)	Mg (MgO)	Al (Al ₂ O ₃)	Si (SiO ₂)	K (Feldspar)	Ca (Wollastonite)	Ti	Fe (Metal)	Total
Spectrum 1	5.16	50.13	0.21	0.77	14.03	19.39	7.37	0.22	0.49	2.23	100.00
Spectrum 2	5.64	56.31	0.24	2.41	8.51	19.21	2.33	0.37	0.40	4.59	100.00
Spectrum 3	6.75	53.67	0.12	1.55	8.65	20.76	3.62	0.17	0.33	4.38	100.00
Mean	5.85	53.37	0.19	1.57	10.40	19.79	4.44	0.25	0.41	3.73	100.00
Std. deviation	0.81	3.10	0.06	0.82	3.15	0.85	2.62	0.10	0.08	1.31	
Max.	6.75	56.31	0.24	2.41	14.03	20.76	7.37	0.37	0.49	4.59	
Min.	5.16	50.13	0.12	0.77	8.51	19.21	2.33	0.17	0.33	2.23	

landfills. These limits are based on total concentration limits for the organic components and pH, as well as leachable components (Environment Agency 2013). The obtained results are summarised in Tables 2 and 3. For all of the evaluated parameters, the obtained results from chemical analysis are below the set limits, except the values of pH and total dissolved solids (TDS) that lay above the WAC limits for inert waste landfill.

5 Grain Size Analysis

The particle size distribution (PSD) curve for natural samples was obtained from wet sieving and hydrometer sedimentation tests according to BS1377:Part2:1990. As shown in Fig. 10 and Table 4, the percentage by weight of fine grains (clay and very fine silt) appears to be larger for Sheppey LC in comparison with shallow depth T5 LC. Using GRADISTAT statistical package (Blott and Pye 2001), further grain size parameters such as sand, silt, and clay contents, texture, mean, mode, median, skewness, sorting, D₁₀, D₂₅, D₅₀, D₇₅, and D₉₀ values were derived as shown in Table 4.

6 Index Properties

Laboratory determination of index parameters carried out according to BS1377:Part2:1990, confirmed a

Table 2 Criteria for granular waste acceptable at landfills—Organic components and pH

Parameter	Unit	Result	WAC limits		
			Inert waste landfill	Stable Non-reactive hazardous landfill	Hazardous waste landfill
Total organic carbon	%	< 1.0	3	5	6
Loss on ignition	%	5.2	–	–	10
BTEX ^a (sum)	mg/kg	< 0.3	6	–	–
PCB's ^b (7 congeners)	mg/kg	< 0.03	1	–	–
Mineral oil > C10–C40	mg/kg	< 16.1	500	–	–
PAH ^c	mg/kg	< 1.7	100	–	–
pH	–	7.7	–	> 6	–

a–Volatile aromatic hydrocarbons benzene, toluene, ethylbenzene and xylenes

b–Polychlorinated biphenyls

c–Polycyclic aromatic hydrocarbons

range of 19–24% and 70–78% respectively for plastic limit (w_p) and liquid limit (w_L) indices. The upper band values are closely matched with $w_p = 28\%$ and $w_L = 77\%$ reported by Jardine et al. (2003) for Sheppey LC. Overall, the plastic limit of Sheppey LC at shallow depths appears to be less than shallow depth T5 LC with $w_p = 29\%$ for Unit C, whereas, the plasticity index for Sheppey LC ($I_p = 52$) is higher than Unit C T5 LC ($I_p = 37$). Based on the unified soil classification system (USCS), Sheppey LC is classified as clay of high plasticity (CH). Based on BS1377:Part2:1990, the specific gravity (G_s) was measured as 2.67 which is lower than the average value of 2.74 reported for Unit C T5 LC (Gasparre 2005).

6.1 Permeability and Water Content

The coefficient of vertical permeability (k_v) was determined based on the constant head test in a triaxial cell (BS1377:Part6:1990). An undisturbed specimen with a diameter of $d = 100$ mm, height of $L = 99$ mm, initial bulk density of $\rho_b = 1.894$ Mg/m³, and initial moisture content of $w_0 = 32.2\%$, was saturated for 7 days and then consolidated for 3 days under an effective stress of 100 kPa. A constant hydraulic gradient of $i = 20$ kPa was applied across the specimen, and the mean rate of flow of water through the soil specimen (Q) was measured (in mL/min). The value of k_v at 20 °C was calculated as 2.5×10^{-10} ms⁻¹ using the Eq. 1;

$$k_v = \frac{1.63QL}{A(i - p_c)} \times R_t \times 10^{-4} \quad (1)$$

where A is the specimen's cross sectional area (in mm²), p_c is the pressure loss in the system (in kPa) for the rate of flow q , and R_t is the temperature correction factor for the viscosity of water.

The in-situ water content was measured in a range of 29–35% based on oven drying method (BS1377:Part2:1990). The Sheppey LC appears to be wetter in comparison with T5 LC having an average in-situ water content of 24–27% at about 7 m depth (Unit C) as reported in Hight et al. (2003) and Gasparre (2005). The moisture condition value (MCV) at the natural moisture content was also measured as 13.2 based on the method described in BS1377:Part4:1990. This parameter is often used for assessment of the condition of a soil, for example, its suitability for use in earthwork construction.

7 One-Dimensional Compression Behaviour

Figure 11a presents a comparison of the normalised compression curves for Sheppey LC and the natural LC from Unit C of T5 site. As the plasticity of the LC deposits increases from west to east of the London basin (Hight et al. 2007), the compression curve for Sheppey specimen was expected to lay below the compression curve for T5 specimen. It is observed that the T5 specimen is less compressible than the Sheppey specimen, mainly due to its lower plasticity index

Table 3 Criteria for granular waste acceptable at landfills—Leachate

Parameter	Unit	Result	WAC limits		
			Inert waste landfill	Stable non-reactive hazardous landfill	Hazardous waste landfill
As (arsenic)	mg/kg	< 0.01	0.5	2	25
Ba (barium)	mg/kg	< 0.02	20	100	300
Cd (cadmium)	mg/kg	< 0.01	0.04	1	5
Cr (chromium (total))	mg/kg	< 0.01	0.5	10	70
Cu (copper)	mg/kg	< 0.04	2	50	100
Hg (mercury)	mg/kg	< 0.01	0.01	0.2	2
Mo (molybdenum)	mg/kg	< 0.01	0.5	10.0	30
Ni (nickel)	mg/kg	< 0.01	0.4	10.0	40
Pb (lead)	mg/kg	< 0.04	0.5	10.0	50
Sb (antimony)	mg/kg	< 0.01	0.06	0.7	5
Se (selenium)	mg/kg	0.04	0.1	0.5	7
Zn (zinc)	mg/kg	< 0.04	4	50	200
Cl (chloride)	mg/kg	249	800	15,000	25,000
F (fluoride)	mg/kg	1	10	150	500
SO ₄ (sulphate)	mg/kg	836	1000	20,000	50,000
Total dissolved solids (TDS) +	mg/kg	4804	4000	60,000	100,000
Phenol index	mg/kg	< 0.4	1	–	–
Dissolved organic carbon	mg/kg	10	500	800	1000

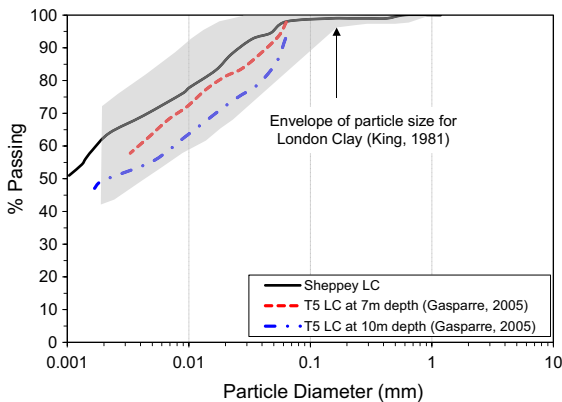


Fig. 10 Particle size distribution curve

($I_p = 37$) and initial water content ($w_0 = 24\%$). Average compression index (C_c) and swelling index (C_s) values of respectively 0.22 and 0.10 were obtained from the compression tests on intact Sheppey specimens having an average initial void ratio of $e_0 = 0.85$. Similar values are derived from the compression curve of the intact T5 specimen.

It is worth mentioning here that soil structure can be disturbed during the process of sampling, transport, and storage, modifying initial properties of the soil sample. Among various soils sampling techniques, block sampling (employed in this study) is considered as a suitable method, which if performed adequately can produce ‘class 1’ quality samples of natural clays with minimum to negligible level of disturbance to the soil structure. Using this method, soil properties such as particle size, water content, density, density index, permeability, compressibility, and shear strength can remain unchanged (BS-EN-1997:2 2007). Furthermore, block samples allow for reliable determination of porosity. Accordingly, the laboratory void ratio values obtained from block samples are, with good accuracy, comparable to the field void ratio.

Figure 11b presents a comparison of the normalised compression curves for reconstituted Sheppey LC and the reconstituted T5 LC. The reconstituted specimens were obtained from consolidation of soil slurry in a Perspex consolidometer under a vertical stress of 80 kPa for a duration of 5 days. Average C_c^* and C_s^* values of respectively 0.38 and 0.13 were

Table 4 Statistical and grain size parameters

Soil Parameter	Sheppey LC		Heathrow T5 LC	
	μm	φ	μm	φ
Mode 1	1.350	9.534	1.790	9.129
Mode 2	9.550	6.713	7.740	7.031
Mode 3	55.000	4.200	57.580	4.123
D ₁₀	1.374	4.204	1.828	4.583
Median or D ₅₀	4.548	7.780	8.150	6.939
D ₉₀	54.250	9.507	41.730	9.095
(D ₉₀ /D ₁₀)	39.490	2.261	22.830	1.985
(D ₉₀ -D ₁₀)	52.880	5.303	39.910	4.513
(D ₇₅ /D ₂₅)	12.950	1.658	5.712	1.448
(D ₇₅ -D ₂₅)	18.860	3.695	16.810	2.514
Mean (\bar{x})*	6.374 ^a	7.294 ^b	8.700	6.845
Sorting (σ)*	4.179 ^a	2.063 ^b	2.996	1.583
Skewness (Sk)*	0.538 ^a	- 0.538 ^b	0.193	-0.193
Kurtosis (K)*	2.060 ^a	2.060 ^b	2.059	2.059
Mean (\bar{x})**	6.827 ^a	7.194 ^b	7.963	6.973
Sorting (σ **	4.286 ^a	2.100 ^b	3.302	1.723
Skewness (Sk **	0.350 ^a	- 0.350 ^b	0.041	- 0.041
Kurtosis (K **	0.607 ^a	0.607 ^b	0.811	0.811
% Coarse Sand	0.2		0.0	
% Medium Sand	0.6		0.0	
% Fine Sand	0.6		0.4	
% Very Fine Sand	0.9		1.6	
% Very Coarse Silt	18.4		13.3	
% Coarse Silt	8.6		16.6	
% Medium Silt	14.4		19.7	
% Fine Silt	8.5		21.9	
% Very Fine Silt	13.9		11.3	
% Clay	33.9		15.2	

*Method of moments (Krumbein and Pettijohn 1938)

**Folk and Ward (1957) Method

^aGeometric values, ^bLogarithmic values

obtained from reconstituted specimens with $e_0 = 0.93$. The reconstituted T5 specimen, with average C_c^* and C_s^* values of respectively 0.39 and 0.15 (Gasparre, 2005), exhibits higher compressibility in comparison with the reconstituted Sheppey specimen.

As reported in Rezanian et al. (2019), the maximum value of creep index (C_α) for Sheppey LC falls approximately in the range of 0.007–0.008 and 0.012–0.013 respectively for intact and reconstituted specimens, the latter being comparable with the

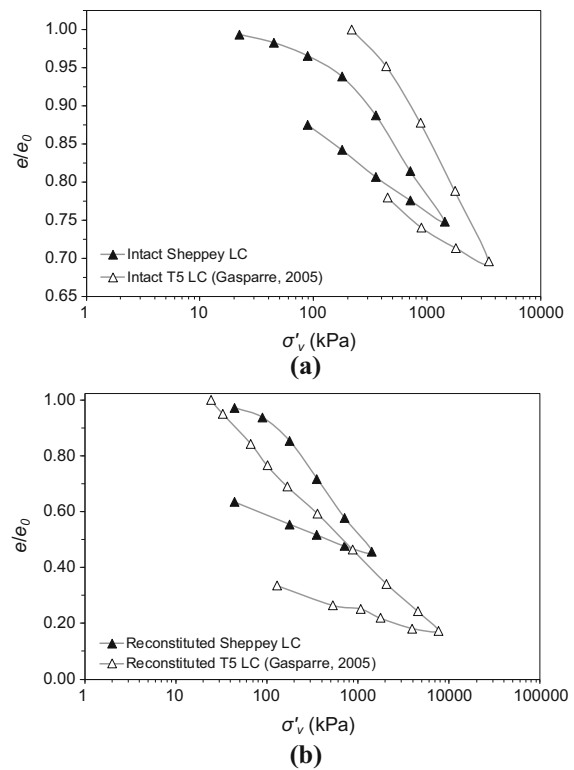


Fig. 11 Comparison of the compression curves for Sheppey LC and T5 LC **a** intact specimens, **b** reconstituted specimens

average value of $C_\alpha = 0.016$ reported by Sorensen (2006) for reconstituted T5 LC. The ratio $\alpha = C_\alpha/C_c$ for Sheppey LC falls approximately in the range of 0.015–0.046 and 0.023–0.037 respectively for intact and reconstituted specimens. The maximum values of α occur at stress levels in a range of 1–2 times yield vertical net stress (σ_p), for both intact and reconstituted specimens.

A series of drained constant rate of strain (CRS) compression-relaxation tests was performed on reconstituted Sheppey LC using an innovative CRS oedometer cell (Bagheri et al. 2020) equipped with two high-capacity tensiometers (Bagheri et al. 2018) for monitoring pore-water pressure evolutions, in order to evaluate the rate-dependent and stress-relaxation responses. Specimens of different initial water contents (and hence different initial suction s_0) were loaded to a certain stress level ($\sigma_0 = 3450$ kPa), then allowed for stress relaxation at zero rate of axial displacement for a minimum time period of 210 h. Table 5 outlines the details of these tests and Fig. 12 presents the soil water retention curve (SWRC) of the

reconstituted soil sample. The SWRC was obtained using HCT technique and following the dynamic method as described in Bagheri (2018). Figure 13 presents the 1D compression behaviour of the specimens loaded at two different strain rates of $\dot{\epsilon}_{v1} = 4.8 \times 10^{-7} \text{ s}^{-1}$ and $\dot{\epsilon}_{v2} = 2.4 \times 10^{-6} \text{ s}^{-1}$, where $\dot{\epsilon}_{v2} = 5 \dot{\epsilon}_{v1}$, in axial strain (ϵ_a) versus vertical net stress (σ_{vnet}) space. The values of the yield vertical net stress (σ_p) were found to decrease exponentially with increase of w_0 for both selected strain rates as shown in Fig. 14.

The values of the coefficient of stress relaxation (R_σ), being the rate of change of σ_{vnet} with time (t) at zero strain rate in log–log space, fell within a range of 0.011–0.019 and 0.017–0.029, respectively for fast and slow strain rates (Bagheri et al. 2019), the latter corresponds well with the values of α ratio of 0.023–0.030 obtained from multi-staged loading

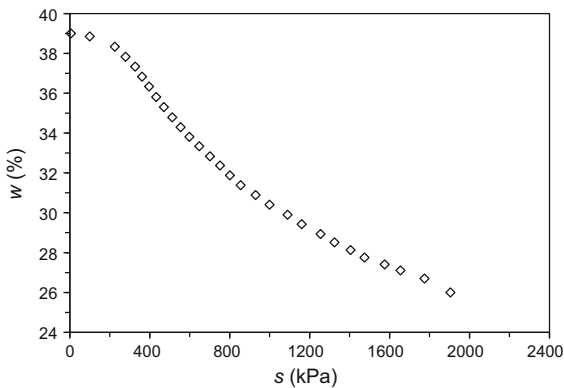
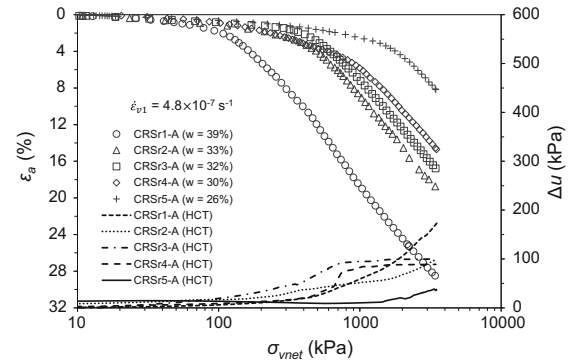
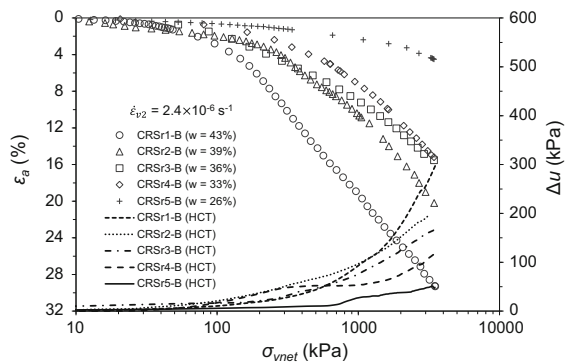


Fig. 12 SWRC for reconstituted soil sample (data from Bagheri 2018)

oedometer tests on reconstituted Sheppey LC at different initial water contents reported in Bagheri (2018).



(a)



(b)

Fig. 13 CRS compression curves at different initial water contents: **a** $\dot{\epsilon}_{v1} = 4.8 \times 10^{-7} \text{ s}^{-1}$, **b** $\dot{\epsilon}_{v2} = 2.4 \times 10^{-6} \text{ s}^{-1}$ (replotted from Bagheri et al. 2019)

Table 5 Details of the CRS tests (data from Bagheri et al. 2019)

Test ID	w_0 [%]	s_0 [kPa]	$\dot{\epsilon}_v$ [s^{-1}]	σ_p [kPa]	σ_o [kPa]
CRSr1-A	39	0	4.8×10^{-7}	157	3451
CRSr2-A	33	701	4.8×10^{-7}	436	3422
CRSr3-A	32	802	4.8×10^{-7}	539	3440
CRSr4-A	30	1045	4.8×10^{-7}	676	3448
CRSr5-A	26	1905	4.8×10^{-7}	1493	3459
CRSr1-B	43	0	2.4×10^{-6}	108	3488
CRSr2-B	39	0	2.4×10^{-6}	227	3451
CRSr3-B	36	433	2.4×10^{-6}	288	3445
CRSr4-B	33	701	2.4×10^{-6}	655	3442
CRSr5-B	26	1905	2.4×10^{-6}	1551	3444

r–reconstituted; A and B–strain rates

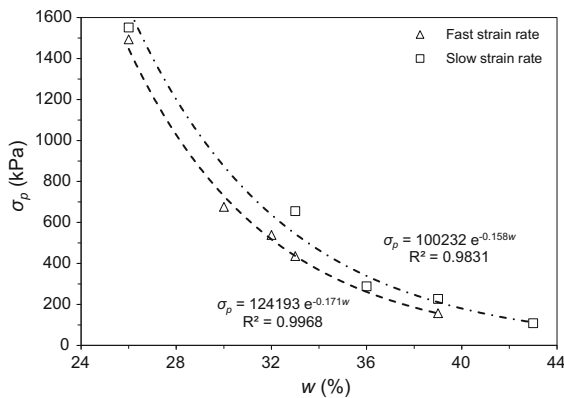


Fig. 14 Variation of σ_p with initial water content (data from Bagheri et al. 2019)

8 Conclusions

Some characteristics of LC from New Hook farm in the Isle of Sheppey were discussed and compared with shallow depth (Unit C) T5 LC. The following conclusions can be drawn;

- The ESEM analyses showed that similar to Unit C T5 LC, Sheppey LC has an open structure containing a large proportion of silt-sized grains which is consistent with PSD of this soil.
- This soil fabric for Sheppey LC is comparable with flocculated cardhouse fabric for T5 LC at shallow depths.
- Silicon dioxide (SiO_2), Aluminium oxide (Al_2O_3), Calcium carbonate (CaCO_3), and Iron disulphide (FeS_2) are predominant constituents of the Sheppey LC.
- The Sheppey LC at shallow depths appears to be wetter and more plastic than shallow depth T5 LC.
- The Sheppey LC is more compressible than the Unit C T5 LC in undisturbed state, and less compressible in reconstituted state.

Open Access This article is licensed under a Creative Commons Attribution 4.0 International License, which permits use, sharing, adaptation, distribution and reproduction in any medium or format, as long as you give appropriate credit to the original author(s) and the source, provide a link to the Creative Commons licence, and indicate if changes were made. The images or other third party material in this article are included in the article's Creative Commons licence, unless indicated otherwise in a credit line to the material. If material is not included in the article's Creative Commons licence and your intended use is not permitted by statutory regulation or exceeds the permitted use, you will need to obtain permission directly

from the copyright holder. To view a copy of this licence, visit <http://creativecommons.org/licenses/by/4.0/>.

References

- Aidiss DT (2014) The stratigraphical framework for the Palaeogene successions of the London Basin, UK. British Geological Survey Open Report OR/14/008
- Bagheri M (2018) Experimental investigation of the time- and rate-dependent behaviour of unsaturated clays. Ph.D. thesis, University of Nottingham
- Bagheri M, Mousavi Nezhad M, Rezaia M (2020) A CRS oedometer cell for unsaturated and non-isothermal tests. *Geotech Test J* 43(1):20180204. <https://doi.org/10.1520/GTJ20180204>
- Bagheri M, Rezaia M, Mousavi Nezhad M (2018) Cavitation in high-capacity tensiometers: effect of water reservoir surface roughness. *Geotech Res* 5(2):81–95. <https://doi.org/10.1680/jgere.17.00016>
- Bagheri M, Rezaia M, Mousavi Nezhad M (2019) Rate-dependency and stress relaxation of unsaturated clays. *Int J Geomech* 19(12):04019128. [https://doi.org/10.1061/\(ASCE\)GM.1943-5622.0001507](https://doi.org/10.1061/(ASCE)GM.1943-5622.0001507)
- Blott SJ, Pye K (2001) GRADISTAT: a grain size distribution and statistics package for the analysis of unconsolidated sediments. *Earth Surf Processes Landf* 26:1237–1248. <https://doi.org/10.1002/esp.261>
- BS1377 (1990) Methods of test for soils for engineering purposes, Part 2: Classification tests
- BS1377 (1990) Methods of test for soils for engineering purposes, Part 4: Compaction related tests
- BS-EN-1997:2 (2007) Eurocode 7—Geotechnical design—Part 2: Ground investigation and testing. London: British Standards Institution
- Burland JB (1990) On the compressibility and shear strength of natural clays. *Géotechnique* 40:329–378
- Burnett AD, Fookes PG (1974) A regional engineering geological study of the London Clay in the London and Hampshire basins. *Q J Eng Geol Hydrogeol* 7:257–295. <https://doi.org/10.1144/GSL.QJEG.1974.007.03.02>
- Environment Agency (2013) Waste sampling and testing for disposal to landfill, Report No. EBPRI 11507B
- Folk RL, Ward WC (1957) Brazos river bar: a study in the significance of grain size parameters. *J Sediment Res* 27:3–26
- Gasparre A (2005) Advanced laboratory characterisation of London Clay. Ph.D. Thesis, University of London
- Helsey M, Codd F (2014) Aviation: proposals for an airport in the Thames Estuary, 1945–2014. House of commons library, standard note SN/BT/4920, pp. 70
- Hight DW, Jardine RJ (1993) Small strain stiffness and strength characteristics of hard London Clay Tertiary clays. International symposium on hard soils-soft rocks, Anagnostopoulos et al. (eds), Athens, Greece. Rotterdam: Balkema, 522–533
- Hight DW, Gasparre A, Nishimura S, Minh NA, Jardine RJ, Coop MR (2007) Characteristics of the London Clay from the Terminal 5 site at Heathrow Airport. *Géotechnique* 57:3–18

- Hight DW, Higgins KG, Jardine RJ, Potts DM, Pickles AR., De Moor EKD, Nyirenda ZM (1993) Predicted and measured tunnel distortions associated with construction of Waterloo international terminal. Predictive soil mechanics: proceedings of the worth memorial symposium, St Catherine's College, Oxford, Houlsby GT, Schofield AN (eds), Thomas Telford, London, 317–338
- Hight DW, Mcmillan F, Powell JJM, Jardine RJ, Allenou CP (2003) Some characteristics of London Clay. In: Proceedings of the 1st international workshop on characterisation and engineering properties of natural soils, Singapore, Tan TS, Phoon KK, Hight KW, Leroueil S, Balkema AA (eds), 851–907
- Huggett JM (1994) Diagenesis of mudrocks and concretions from the London clay formation in the London basin. *Clay Miner* 29:693–707
- Jardine RJ, Smith PR, Nicholson DP (2003) Properties of the soft Holocene Thames Estuary Clay from Queenborough, Kent. *In: Proceedings of the 1st International workshop on characterisation and engineering properties of natural soils, Paris*, Tan TS, Phoon KK, Hight DW, Leroueil S, Balkema AA (eds), 599–643
- Jardine RJ (1985) Investigations of pile-soil behaviour, with special reference to the foundations of offshore structures. PhD Thesis, University of London (Imperial College).
- King C (1981) The stratigraphy of the London Clay and associated deposits. Tertiary Research Special Paper, Backhuys, Rotterdam
- Rezania M, Bagheri M, Mousavi Nezhad M (2020) Creep and consolidation of a stiff clay under saturated and unsaturated conditions. *Can Geotech J* 57(5):728–741
- Skempton AW, Schuster FRS, Petley DJ (1969) Joints and fissures in the London Clay at Wraybury and Edgware. *Géotechnique* 19:205–217
- Smith PR (1992) The properties of natural high compressibility clays with particular reference to construction on soft ground. PhD Thesis, University of London (Imperial College)
- Sorensen KK (2006) Influence of viscosity and ageing on the behaviour of clays. Ph.D. Thesis, University College London

Publisher's Note Springer Nature remains neutral with regard to jurisdictional claims in published maps and institutional affiliations.